Assessment of Hepatic Perfusion Using GRASP MRI
Bringing Liver MRI on a New Level

Jakob Weiss, MD, Christer Ruff, MD, Ulrich Grosse, MD, Gerd Grözinger, MD, Marius Horger, MD, Konstantin Nikolaou, MD, and Sergios Gatidis, MD

Purpose: The aim of this study was to demonstrate the feasibility of hepatic perfusion imaging using dynamic contrast-enhanced (DCE) golden-angle radial sparse parallel (GRASP) magnetic resonance imaging (MRI) for characterizing liver parenchyma and hepatocellular carcinoma (HCC) before and after transarterial chemoembolization (TACE) as a potential alternative to volume perfusion computed tomography (VPCT).

Methods and Materials: Between November 2017 and September 2018, 10 patients (male = 8; mean age, 66.5 ± 8.6 years) with HCC were included in this prospective, institutional review board–approved study. All patients underwent DCE GRASP MRI with high spatiotemporal resolution after injection of liver-specific MR contrast agent before and after TACE. In addition, VPCT was acquired before TACE serving as standard of reference. From the dynamic imaging data of DCE MRI and VPCT, perfusion maps (arterial liver perfusion [mL/100 mL/min], portal liver perfusion [mL/100 mL/min], hepatic perfusion index [%]) were calculated using a dual-input maximum slope model and compared with assess perfusion measures, lesion characteristics, and treatment response using Wilcoxon signed-rank test. To evaluate interreader agreement for measurement repeatability, the interclass correlation coefficient (ICC) was calculated.

Results: Perfusion maps could be successfully generated from all DCE MRI and VPCT data. The ICC was excellent for all perfusion maps (ICC ≥ 0.88; $P \leq 0.001$). Image analyses revealed perfusion parameters for DCE MRI and VPCT within the same absolute range for tumor and liver tissue. Dynamic contrast-enhanced MRI further enabled quantitative assessment of treatment response showing a significant decrease ($P \leq 0.01$) of arterial liver perfusion and hepatic perfusion index in the target lesion after TACE.

Conclusions: Dynamic contrast-enhanced GRASP MRI allows for a reliable and robust assessment of hepatic perfusion parameters providing quantitative results comparable to VPCT and enables characterization of HCC before and after TACE, thus posing the potential to serve as an alternative to VPCT.

Key Words: liver MRI, perfusion imaging, hepatocellular carcinoma, maximum slope model

(*Invest Radiol* 2019;54: 737–743)

Multiphase contrast-enhanced magnetic resonance imaging (MRI) is a cornerstone for the assessment of liver pathologies.[1] Analysis of perfusion patterns not only allows for characterization and identification of hepatic lesions but also plays an important role for the assessment of therapy response of systemic and local therapies including transarterial chemoembolization (TACE).[2–4]

In clinical routine, MRI examinations of the liver usually include measurements at different intervals before and after the administration of intravenous contrast agent aiming to depict the hepatic perfusion state at distinct time points during arterial, portal venous, and late phases.[5] This approach has the limitation of a relatively low temporal resolution and susceptibility to respiratory motion artifacts.[6] Thus, it is not possible to reliably extract dynamic data that allow for a reproducible quantitative analysis of hepatic perfusion.[7]

In contrast, volume perfusion computed tomography (VPCT) has been established as the standard of reference for whole-organ perfusion analysis of the liver.[8] Specifically for characterizing and analyzing perfusion kinetics of hepatocellular carcinomas (HCCs), VPCT offers reliable quantitative data due to a very high temporal resolution that is necessary for accurate measurements.[9–11]

Recently, golden-angle radial sparse parallel (GRASP) MRI has been introduced as a rapid and motion-robust technique combining radial k-space sampling and iterative reconstruction allowing for dynamic contrast-enhanced (DCE) MRI of the liver with a spatiotemporal resolution similar to CT.[12,13] This advance provides the technological basis for MR-based quantification of liver perfusion.[14] Furthermore, potential advantages GRASP MRI compared with VPCT are lack of ionizing radiation, robustness against radiopaque materials (eg, lipiodol deposits after TACE), comprehensive multiparametric imaging in combination with additional imaging sequences, and combination with liver-specific contrast agents.

Therefore, the purpose of this study was to demonstrate the feasibility of hepatic perfusion imaging using DCE GRASP MRI for characterizing liver parenchyma and HCC before and after TACE as a potential alternative to VPCT.

METHODS AND MATERIALS

Study Cohort and Design

Between November 2017 and September 2018, 13 patients with known HCC were consecutively included in this prospective, institutional review board–approved study. All patients were scheduled for TACE based on an interdisciplinary tumor board decision, and underwent DCE MRI and VPCT before the intervention and received DCE MRI control imaging after the intervention. All examinations were performed within 2 days before/after treatment.

Three patients had to be excluded due to extravasation of contrast agent (n = 1), severe motion artifacts (n = 1), and administration of a different contrast agent (n = 1) resulting in a final cohort of 10 patients (male = 8; mean age, 66.5 ± 8.6 years; see also Table 1).

Image Acquisition and Reconstruction

Dynamic Contrast-Enhanced Magnetic Resonance Imaging

All MR examinations were performed on a 3 T System (MAGNETOM Vida; Siemens Healthineers, Germany) with patients in supine position. To reduce streak artifacts, arms were moved overhead. Dynamic contrast-enhanced MRI was performed using a fat-saturated, T1-weighted gradient echo sequence with a GRASP sampling scheme.[12] Image data were continuously acquired for 5 minutes. Twenty seconds after the start of data acquisition, hepatocyte-specific contrast agent (0.025 mmol/kg body weight, Gd-EOB-DTPA, Bayer, Healthcare, Germany) was administered through a cubital vein at a flow rate of 2 mL/s followed by a saline flush (20 mL, 2 mL/s).

Received for publication March 19, 2019; and accepted for publication, after revision, April 18, 2019.
From the Department of Diagnostic and Interventional Radiology, Eberhard Karls University, Tuebingen, Germany.
Conflicts of interest and sources of funding: none declared.
Correspondence to: Jakob Weiss, MD, Department of Diagnostic and Interventional Radiology, University of Tuebingen, Hoppe-Seyler-Str. 3, 72076 Tuebingen, Germany. E-mail: Jakob.Weiss@uni-tuebingen.de.

ISSN: 0020-9996/19/5412–0737
DOI: 10.1097/RLI.0000000000000586

TABLE 1. Patient Demographics and Acquisition Parameters of DCE GRASP MRI and VPCT

Variables	
Patient demographics	
Age, mean ± SD, y	66.5 ± 8.6
Sex, male/female	8/2
Known liver disease	10
Hepatitis C	4
Nutritive toxic	4
Hepatitis B	1
Hemochromatosis	1
Child-Pugh score	n = 8 (A); n = 2 (unknown)
Cancer diagnosis	Hepatocellular carcinoma
GRASP MRI	
TR, ms	2.86
TE, ms	1.26
Flip angle, degree	12.5
Voxel size, mm	1.5 × 1.5 × 3
Matrix, mm^2	256 × 256
Bandwidth, Hz/s	930
Temporal resolution, s	1.7
Scan time, s	318
Covered time interval for perfusion maps, s	~90
No. time points	55
VPCT	
kV	80
mAs	140
Collimation, mm	0.6
Voxel size, mm	1.3 × 1.3 × 3
Matrix, mm^2	512 × 512
Temporal resolution, s	1.5
Covered time interval, s	~90
No. time points	24

GRASP indicates golden-angle radial sparse parallel; MRI, magnetic resonance imaging; VPCT, volume perfusion computed tomography; TR, repetition time; TE, echo time; kV, tube voltage; mAs, tube current time product.

From the raw data, a series with a temporal resolution of 1.7 seconds was reconstructed. For reasons of comparability, we only used data from the first 90 seconds after detection of contrast agent in the aorta for image reconstruction to mimic the time interval covered by the CT protocol (see below, Table 1 and Fig. 1). The temporal resolution and time intervals between the individual time points were kept constant for the entire dataset. For calculation of absolute contrast agent concentrations, B1-corrected T1-maps were generated using the dual flip angle method and B1-mapping as previously described.[15]

From this time-resolved contrast agent concentration series, parametric perfusion maps were calculated (arterial liver perfusion = ALP [mL/100 mL/min], portal liver perfusion = PVP [mL/100 mL/min], hepatic perfusion index = HPI [%]) using an in-house developed Matlab script (Version 2014b; Mathworks) by applying the model-free direct dual input maximum slope approach using the following equations[16]:

$$ALP = \frac{G_{art}}{I_{aorta}} PVP = \frac{G_{portal}}{I_{portal}v} HPI = \frac{ALP}{ALP + PVP}$$

where ALP indicates hepatic arterial perfusion; G_art, peak hepatic arterial phase gradient; I_aorta, peak aortic enhancement; PVP, portal venous perfusion; G_portal, peak hepatic portal venous phase gradient; I_portal_v, peak portal vein enhancement; and HPI, hepatic perfusion index.

Volume Perfusion Computed Tomography

Volume perfusion computed tomography examinations were performed on second-generation dual-source CT system (SOMATOM Definition Flash; Siemens Healthineers, Germany) with a *z*-axis scan coverage between 11.4 and 17.6 cm in adaptive spiral scanning technique. After a scan delay of 7 seconds, 50 mL of contrast agent (Ultravist 370; Bayer, Germany) were administered through a cubital vein at a flow rate of 5 mL/s followed by a saline flush (50 mL, 5 mL/s).

Subsequently, perfusion maps (ALP, PVP, HPI) were calculated using the same mathematical approach as described previously for DCE MRI with dedicated, vendor-provided postprocessing software (Syngo Volume Perfusion CT Body; Siemens Healthineers, Germany). Further detailed acquisition parameters for DCE MRI and VPCT are given in Table 1.

Figure 1 depicts an example of time-intensity curves (aorta, portal vein, spleen, liver parenchyma, and HCC) derived from GRASP MRI and VPCT in the same patient.

Image Analysis

Perfusion parameters were measured in ALP, PVP, and HPI maps using Osirix (Pixmeo, Version 10.0.1; Switzerland). To evaluate interreader agreement for measurement repeatability, 2 readers with 5 (JW) and 7 (SG) years of experience in MRI independently performed measurements in all perfusion maps. At first, circular region of interest (ROI) were placed in the target lesion in the HPI map of DCE MRI within the axial slice of maximum lesion size without involving adjacent liver. In addition, a circular ROI was placed in normal liver tissue. Subsequently, ROIs were copied to the remaining ALP and PVP maps in DCE MRI pre- and post-TACE examinations and VPCT maps with slight adaption, where necessary.

Statistical Analyses

Statistical analyses were performed using SPSS (Version 22; IBM, United States). Continuous variables are given as mean ± SD.

Interreader agreement for measurement repeatability was calculated for all perfusion measurements using the interclass correlation coefficient (ICC), which was interpreted as follows: ICC less than 0.2, poor; 0.2 to 0.4, fair; 0.4 to 0.6, moderate; 0.6 to 0.8, substantial; and 0.8 to 1.0, excellent. For further analyses, the mean of the individual reader results was calculated.

Quantitative perfusion measures in DCE MRI and VPCT as well as changes of perfusion parameter in DCE MRI after TACE were compared using the Wilcoxon signed-rank test.

A 2-sided P value below 0.05 was considered as statically significant.

RESULTS

Parametric maps could be generated from all DCE MRI and VPCT data. In pre-TACE studies, 11 HCC lesions were detected in 10 patients in both modalities. Mean lesion size was 35.9 ± 26.5 mm. Imaging examples of pre- and post-TACE DCE MRI and VPCT are given in Figures 2 to 4.

Image Analysis

A summary of ALP, HPI, and PVP measures derived from DCE MRI and VPCT are presented in Table 2. Interreader agreement for measurement repeatability was excellent for all evaluated perfusion maps with an ICC ≥ 0.88 ($P \leq 0.001$).

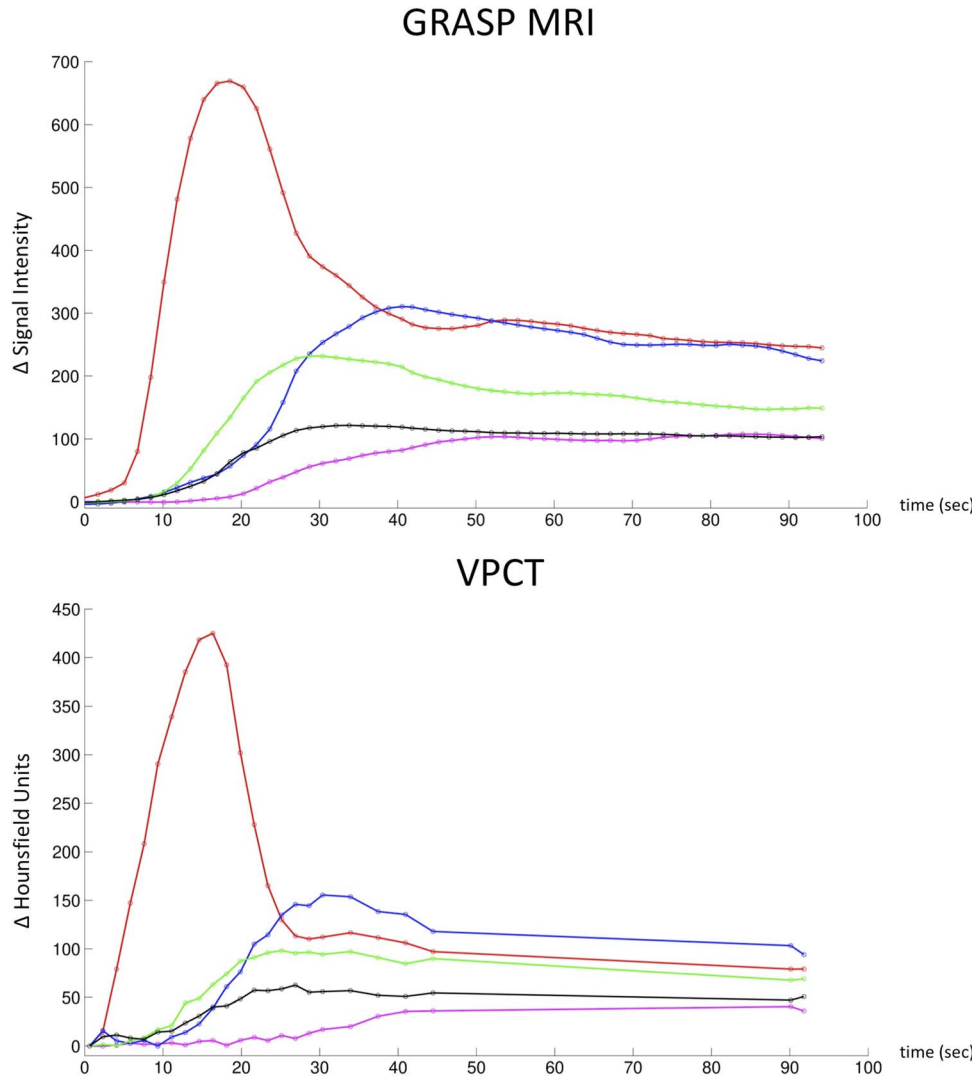

FIGURE 1. Example of perfusion curves in the same patient using GRASP MRI and VPCT. Red indicates aorta; blue, portal vein; green, spleen; violet, liver parenchyma; black, hepatocellular carcinoma. GRASP MRI indicates golden-angle radial sparse parallel MRI; VPCT, volume perfusion computed tomography.

Comparison of DCE MRI and VPCT

In normal liver tissue and before TACE, ALP was found to be slightly but statistically significant higher in DCE MRI than in VPCT (18.9 ± 8.1 vs 10.8 ± 5.5 mL/100 mL/min, $P = 0.005$), whereas HPI (23.3% ± 8.1% vs 21.6% ± 13.6%, $P = 0.57$) and PVP (63.6 ± 12.8 vs 55.3 ± 18.1 mL/100 mL/min, $P = 0.33$) were in the same quantitative range. After TACE, perfusion measures in the DCE MRI were as follows: ALP, 27.9 ± 13.8 mL/100 mL/min; HPI, 26.5% ± 9.8%; and PVP, 83.9 ± 35.1 mL/100 mL/min.

Regarding HCC lesions before TACE, a relative underestimation of HPI was observed in DCE MRI compared with VPCT (79.1% ± 14.9% vs 96.5% ± 3.8%, $P = 0.005$) mainly as a result of overestimating PVP (16.4 ± 12.3 vs 2.9 ± 1.6 mL/100 mL/min, $P = 0.01$), whereas ALP was in the same range in the 2 modalities (55.5 ± 26.0 vs 45.3 ± 9.7 mL/100 mL/min, $P = 0.28$). A summary of all results and pairwise comparison is given in Table 3.

Change of Perfusion Parameters After TACE

In HCC lesions, a significant decrease in ALP from 55.5 ± 26.0 to 16.4 ± 13.7 mL/100 mL/min and in HPI from 79.1% ± 14.9% to 40.4% ± 23.9% was observed after TACE ($P \leq 0.01$; Fig. 4), indicating a treatment effect and a successful delivery of the beads into the target lesion. A summary including results for perfusion changes in liver parenchyma is provided in Table 4.

DISCUSSION

In this study, we investigated the feasibility of DCE GRASP MRI for quantitative perfusion analyses of HCC and liver parenchyma. We found that this approach facilitates a robust calculation of perfusion parameters yielding quantitative results comparable to VPCT-based measures and allows for qualitative and quantitative characterization of HCC before and after TACE.

This is of clinical implication since up till now reliable quantitative perfusion data with high spatial resolution could only be acquired using CT given the high temporal resolution necessary to fit the mathematical requirements of available perfusion models.[7,8] Although VPCT studies have been established as a valuable diagnostic tool in clinical routine, well-known disadvantages are the need of ionizing radiation and iodine contrast agent, which hinders its widespread and repeated application.[17,18] With GRASP, a new era of MR data acquisition and

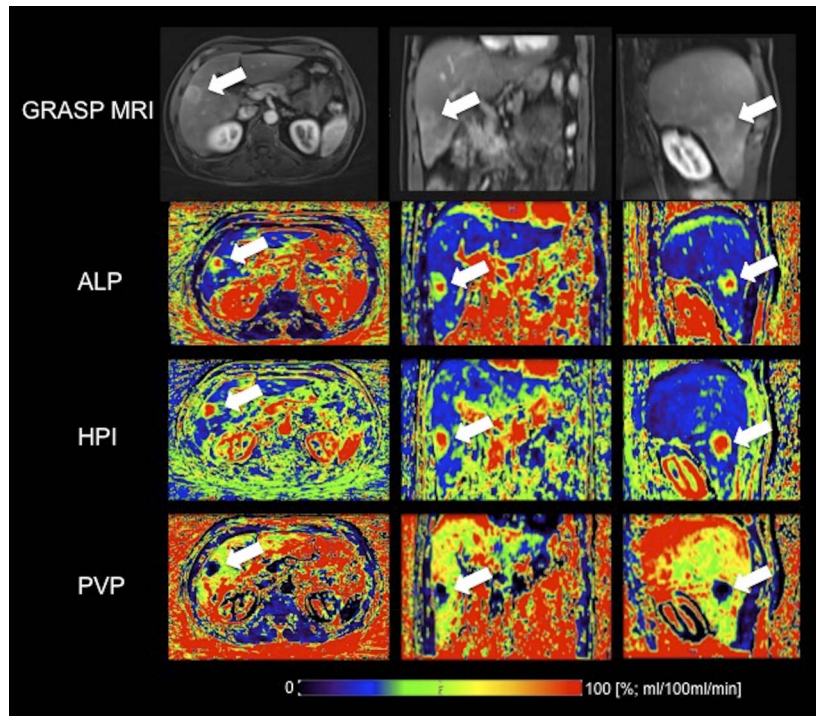

FIGURE 2. Morphological GRASP MRI images and perfusion maps of a 54-year-old male patient with a hepatocellular carcinoma (arrow) before TACE. The target lesion is clearly visible in the arterial phase GRASP MRI images and the perfusion maps. In the lesion periphery, partial volume effects are seen, which may result in underestimation of HPI. GRASP MRI indicates golden-angle radial sparse parallel MRI; TACE, transarterial chemoembolization; ALP, arterial liver perfusion [mL/100 mL/min]; HPI, hepatic perfusion index [%]; PVP, portal liver perfusion [mL/100 mL/min].

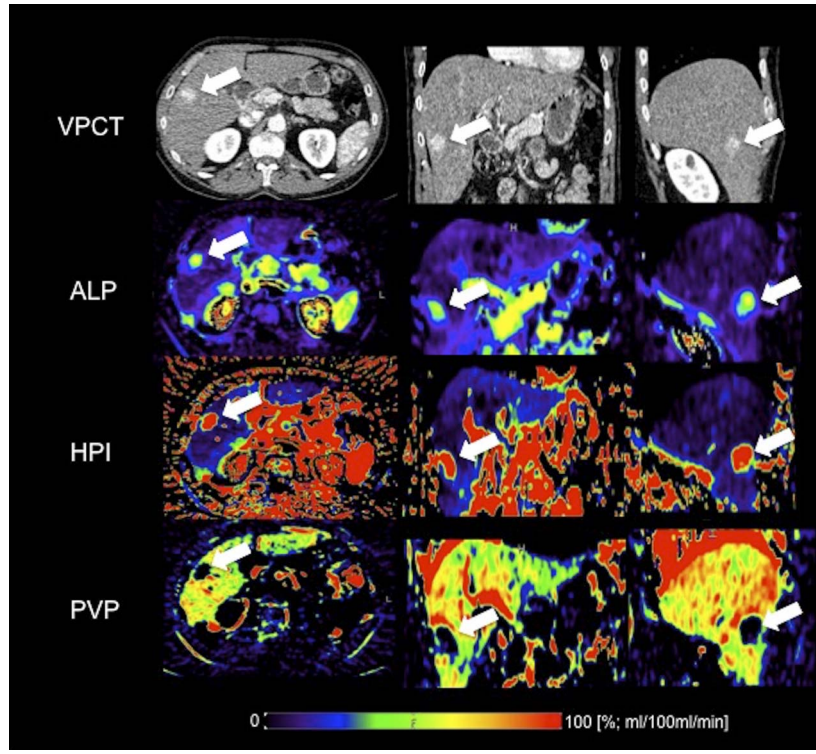

FIGURE 3. Corresponding VPCT images and perfusion maps to Figure 2 of a 54-year-old male patient with a hepatocellular carcinoma (arrow) before TACE. The target lesion is clearly visible in the VPCT images and the perfusion maps. VPCT, volume perfusion computed tomography; TACE, transarterial chemoembolization; ALP, arterial liver perfusion [mL/100 mL/min]; HPI, hepatic perfusion index [%]; PVP, portal liver perfusion [mL/100 mL/min].

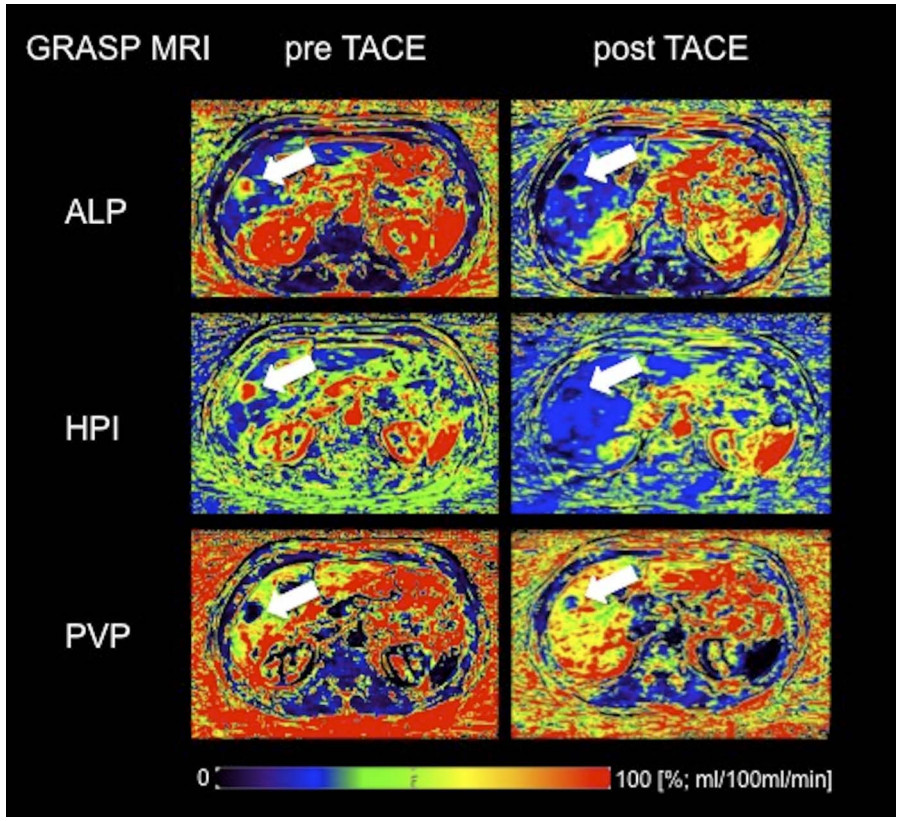

FIGURE 4. Comparison of perfusion maps derived from GRAPS MRI before and after TACE. The target lesion (arrow) shows distinct changes in perfusion characteristics (decrease in ALP and HPI, relative increase in PVP) after treatment. GRASP MRI, golden-angle radial sparse parallel MRI; TACE, transarterial chemoembolization; ALP, arterial liver perfusion [mL/100 mL/min]; HPI, hepatic perfusion index [%]; PVP, portal liver perfusion [mL/100 mL/min].

reconstruction has been introduced that allows for rapid and motion-robust data sampling, which can overcome these drawbacks from VPCT.[12,19]

Golden-angle radial sparse parallel data are continuously acquired during the hepatic contrast agent passage within a standard multiparametric MR examination. Subsequently, images with different temporal resolutions can be reconstructed depending on the particular clinical indication.[14] Calculating images with a relatively low temporal resolution provides high image quality at various time points (arterial, portal venous, and late phases)

TABLE 2. Interreader Agreement

	Reader 1	Reader 2			Reader 1	Reader 2	
GRASP MRI Pre-TACE	**Mean ± SD**	**Mean ± SD**	**ICC**		**Mean ± SD**	**Mean ± SD**	**ICC**
ALP_{tumor}	55.3 ± 26.5	55.8 ± 25.7	0.99	ALP_{liver}	18.8 ± 8.3	19.1 ± 7.6	0.99
HPI_{tumor}	78.9 ± 15.2	79.2 ± 14.8	0.99	HPI_{liver}	23.0 ± 8.6	23.7 ± 7.7	0.99
PVP_{tumor}	16.1 ± 12.3	16.7 ± 12.4	0.99	PVP_{liver}	64.0 ± 12.8	63.2 ± 12.9	0.99
GRASP MRI Post-TACE							
ALP_{tumor}	16.8 ± 14.2	15.9 ± 13.3	0.99	ALP_{liver}	28.3 ± 13.4	27.7 ± 14.2	0.99
HPI_{tumor}	40.5 ± 23.9	40.4 ± 24.0	0.99	HPI_{liver}	26.2 ± 10.2	26.8 ± 9.4	0.99
PVP_{tumor}	24.7 ± 17.2	25.1 ± 16.7	0.99	PVP_{liver}	83.6 ± 35.2	84.2 ± 34.9	0.98
VPCT Pre-TACE							
ALP_{tumor}	45.1 ± 9.7	45.5 ± 7.2	0.99	ALP_{liver}	10.5 ± 5.8	11.2 ± 5.5	0.97
HPI_{tumor}	96.3 ± 3.8	97.6 ± 4.1	0.98	HPI_{liver}	22.1 ± 13.3	21.1 ± 14.0	0.99
PVP_{tumor}	2.6 ± 1.4	3.2 ± 2.0	0.88	PVP_{liver}	55.0 ± 17.9	55.4 ± 18.2	0.98

Summary statistics of the quantitative image analyses pre- and post-TACE for GRASP MRI and VPCT and results of ICC calculation to assess interreader agreement.

GRASP indicates golden-angle radial sparse parallel; MRI, magnetic resonance imaging; VPCT, volume perfusion computed tomography; TACE, transarterial chemoembolization; ALP, arterial liver perfusion [mL/100 mL/min]; HPI, hepatic perfusion index [%]; PVP, portal liver perfusion [mL/100 mL/min].

TABLE 3. Quantitative Image Analysis

Pre-TACE							
	GRASP MRI Mean ± SD	VPCT Mean ± SD	*P*		GRASP MRI Mean ± SD	VPCT Mean ± SD	*P*
ALP_{tumor}	55.5 ± 26.0	45.3 ± 9.7	0.28	ALP_{liver}	18.9 ± 8.1	10.8 ± 5.5	0.005*
HPI_{tumor}	79.1 ± 14.9	96.5 ± 3.8	0.005*	HPI_{liver}	23.3 ± 8.1	21.6 ± 13.6	0.57
PVP_{tumor}	16.4 ± 12.3	2.9 ± 1.6	0.01*	PVP_{liver}	63.6 ± 12.8	55.3 ± 18.1	0.33
Post-TACE							
	GRASP MRI Mean ± SD	VPCT Mean ± SD	*P*		GRASP MRI Mean ± SD	VPCT Mean ± SD	*P*
ALP_{tumor}	16.4 ± 13.7	NA	NA	ALP_{liver}	27.9 ± 13.8	NA	NA
HPI_{tumor}	40.4 ± 23.9	NA	NA	HPI_{liver}	26.5 ± 9.8	NA	NA
PVP_{tumor}	24.9 ± 17.0	NA	NA	PVP_{liver}	83.9 ± 35.1	NA	NA

Summary statistics of mean perfusion measures (mean of reader 1 and reader 2) pre- and post-TACE and comparison between GRASP MRI and VPCT.

*Significant results are indicated with asterisk.

GRASP indicates golden-angle radial sparse parallel; MRI, magnetic resonance imaging; VPCT, volume perfusion computed tomography; TACE, transarterial chemoembolization; ALP, arterial liver perfusion [mL/100 mL/min]; HPI, hepatic perfusion index [%]; PVP, portal liver perfusion [mL/100 mL/min].

suitable for reading in clinical routine.[20] By shortening the temporal resolution (1–2 seconds), the data set can be used to extract quantitative perfusion measures.[14] Moreover, combining GRASP MRI with additional morphological (eg, T2-weighted imaging) and functional (diffusion-weighted imaging) sequences allows for an even more comprehensive assessment of hepatic pathologies. In contrast, VPCT examinations only provide quantitative perfusion maps but no diagnostic images. For auxiliary morphological information, further scans are necessary with the need for additional contrast agent and ionizing radiation. In this context, we consider DCE GRASP MRI as an encouraging approach for quantitative perfusion analysis of the liver, which may serve as a potential alternative to VPCT.

Analysis of perfusion parameters in our study cohort revealed perfusion measures within the same absolute range in DCE MRI and VPCT in our study and in the literature despite substantial differences concerning contrast agent volume and concentrations as well as examinations protocol, thus demonstrating a high robustness of this approach.[10,21] Observed smaller deviations can be in part explained by physiological changes of liver perfusion that can occur, for example, after fasting or food intake and/or different underlying patient characteristics (eg, degree of liver cirrhosis). In addition, a moderate relative underestimation of HPI and overestimation of PVP in HCC lesions was observed in DCE MRI compared with VPCT. We hypothesize that this stems from partial volume effects in the periphery of lesions as no additional motion correction was used for reconstructing GRASP data. A possible solution could be retrospective motion correction for GRASP data reconstruction as described by Feng et al.[19]

Administration of gadolinium-based contrast agents has improved the diagnostic accuracy of liver MRI.[22] However, given their different T1 relaxivity, chemical structure, and dosage recommendations, they differ in terms of enhancement characteristics with potential effects on perfusion parameters. Gadobutrol leads to higher signal intensity changes of liver parenchyma in the arterial and portal venous phase, which can most likely be explained by its higher molar concentration and relaxivity as compared with Gd-EOB-DTPA.[23,24] This might be of particular benefit for the detection of small, hypervascularized liver lesions. In contrast, Gd-EOB-DTPA allows for a more precise assessment of the hepatobiliary structures and liver function and has been proven beneficial to improve detection and characterization of lesions due to its hepatocyte-specific properties.[23,25,26] Consequently, the choice of the contrast agent is always a trade-off considering the individual patient's needs, and more focused studies are necessary to investigate the effect of different contrast agent properties on quantitative hepatic perfusion analysis.

The following limitations need to be addressed. The sample size of this pilot study is relatively small and only focuses on the maximum slope method and HCC lesions. Further investigation and comparison with other perfusion methods (eg, arterial spin labeling) and models as well as diseases are necessary to gain a more comprehensive understanding of MR-based hepatic perfusion analysis and to evaluate their value for clinical decision-making. In addition, no VPCT examinations

TABLE 4. Comparison GRASP MRI Pre- and Post-TACE

	Pre-TACE	Post-TACE			Pre-TACE	Post-TACE	
GRASP MRI	Mean ± SD	Mean ± SD	*P*	GRASP MRI	Mean ± SD	Mean ± SD	*P*
ALP_{tumor}	55.5 ± 26.0	16.4 ± 13.7	0.005*	ALP_{liver}	18.9 ± 8.1	27.9 ± 13.8	0.03*
HPI_{tumor}	79.1 ± 14.9	40.4 ± 23.9	0.01*	HPI_{liver}	23.3 ± 8.1	26.5 ± 9.8	0.39
PVP_{tumor}	16.4 ± 12.3	24.9 ± 17.0	0.24	PVP_{liver}	63.6 ± 12.8	83.9 ± 35.1	0.07

Comparison of mean perfusion measures in GRASP MRI pre- and post-TACE and results of pairwise comparison.

*Significant results are indicated with asterisk.

GRASP indicates golden-angle radial sparse parallel; MRI, magnetic resonance imaging; TACE, transarterial chemoembolization; ALP, arterial liver perfusion [mL/100 mL/min]; HPI, hepatic perfusion index [%]; PVP, portal liver perfusion [mL/100 mL/min].

were available after TACE to compare treatment response among imaging modalities.

In conclusion, DCE GRASP MRI allows for a reliable and robust assessment of hepatic perfusion parameters with high spatiotemporal resolution providing quantitative results comparable to VPCT and enables characterization of HCC before and after TACE, thus posing the potential to serve as an alternative to VPCT.

REFERENCES

1. Fowler KJ, Brown JJ, Narra VR. Magnetic resonance imaging of focal liver lesions: approach to imaging diagnosis. *Hepatology*. 2011;54:2227–2237.
2. Chen BB, Hsu CY, Yu CW, et al. Early perfusion changes within 1 week of systemic treatment measured by dynamic contrast-enhanced MRI may predict survival in patients with advanced hepatocellular carcinoma. *Eur Radiol*. 2017;27:3069–3079.
3. Tamandl D, Waneck F, Sieghart W, et al. Early response evaluation using CT-perfusion one day after transarterial chemoembolization for HCC predicts treatment response and long-term disease control. *Eur J Radiol*. 2017;90:73–80.
4. Elsayes KM, Narra VR, Yin Y, et al. Focal hepatic lesions: diagnostic value of enhancement pattern approach with contrast-enhanced 3D gradient-echo MR imaging. *Radiographics*. 2005;25:1299–1320.
5. Donato H, Franca M, Candelaria I, et al. Liver MRI: from basic protocol to advanced techniques. *Eur J Radiol*. 2017;93:30–39.
6. Pandharipande PV, Krinsky GA, Rusinek H, et al. Perfusion imaging of the liver: current challenges and future goals. *Radiology*. 2005;234:661–673.
7. Cuenod CA, Balvay D. Perfusion and vascular permeability: basic concepts and measurement in DCE-CT and DCE-MRI. *Diagn Interv Imaging*. 2013;94:1187–1204.
8. Kim SH, Kamaya A, Willmann JK. CT perfusion of the liver: principles and applications in oncology. *Radiology*. 2014;272:322–344.
9. Kartalis N, Brehmer K, Loizou L. Multi-detector CT: liver protocol and recent developments. *Eur J Radiol*. 2017;97:101–109.
10. Kaufmann S, Horger T, Oelker A, et al. Characterization of hepatocellular carcinoma (HCC) lesions using a novel CT-based volume perfusion (VPCT) technique. *Eur J Radiol*. 2015;84:1029–1035.
11. Sahani DV, Holalkere NS, Mueller PR, et al. Advanced hepatocellular carcinoma: CT perfusion of liver and tumor tissue—initial experience. *Radiology*. 2007;243:736–743.
12. Chandarana H, Feng L, Block TK, et al. Free-breathing contrast-enhanced multiphase MRI of the liver using a combination of compressed sensing, parallel imaging, and golden-angle radial sampling. *Invest Radiol*. 2013;48:10–16.
13. Chandarana H, Feng L, Ream J, et al. Respiratory motion-resolved compressed sensing reconstruction of free-breathing radial acquisition for dynamic liver magnetic resonance imaging. *Invest Radiol*. 2015;50:749–756.
14. Chandarana H, Block TK, Ream J, et al. Estimating liver perfusion from free-breathing continuously acquired dynamic gadolinium-ethoxybenzyl-diethylenetriamine pentaacetic acid-enhanced acquisition with compressed sensing reconstruction. *Invest Radiol*. 2015;50:88–94.
15. Thng CH, Koh TS, Collins DJ, et al. Perfusion magnetic resonance imaging of the liver. *World J Gastroenterol*. 2010;16:1598–1609.
16. White MJ, O'Gorman RL, Charles-Edwards EM, et al. Parametric mapping of the hepatic perfusion index with gadolinium-enhanced volumetric MRI. *Br J Radiol*. 2007;80:113–120.
17. Brix G, Lechel U, Petersheim M, et al. Dynamic contrast-enhanced CT studies: balancing patient exposure and image noise. *Invest Radiol*. 2011;46:64–70.
18. Gawlitza J, Haubenreisser H, Meyer M, et al. Comparison of organ-specific-radiation dose levels between 70 kVp perfusion CT and standard tri-phasic liver CT in patients with hepatocellular carcinoma using a Monte-Carlo-Simulation-based analysis platform. *Eur J Radiol Open*. 2016;3:95–99.
19. Feng L, Axel L, Chandarana H, et al. XD-GRASP: golden-angle radial MRI with reconstruction of extra motion-state dimensions using compressed sensing. *Magn Reson Med*. 2016;75:775–788.
20. Feng L, Grimm R, Block KT, et al. Golden-angle radial sparse parallel MRI: combination of compressed sensing, parallel imaging, and golden-angle radial sampling for fast and flexible dynamic volumetric MRI. *Magn Reson Med*. 2014;72:707–717.
21. Marquez HP, Karalli A, Haubenreisser H, et al. Computed tomography perfusion imaging for monitoring transarterial chemoembolization of hepatocellular carcinoma. *Eur J Radiol*. 2017;91:160–167.
22. Usman S, Smith L, Brown N, et al. Diagnostic accuracy of magnetic resonance imaging using liver tissue specific contrast agents and contrast enhanced multi detector computed tomography: a systematic review of diagnostic test in hepatocellular carcinoma (HCC). *Radiography (Lond)*. 2018;24:e109–e114.
23. Zizka J, Klzo L, Ferda J, et al. Dynamic and delayed contrast enhancement in upper abdominal MRI studies: comparison of gadoxetic acid and gadobutrol. *Eur J Radiol*. 2007;62:186–191.
24. Budjan J, Ong M, Riffel P, et al. CAIPIRINHA-Dixon-TWIST (CDT)-volume-interpolated breath-hold examination (VIBE) for dynamic liver imaging: comparison of gadoterate meglumine, gadobutrol and gadoxetic acid. *Eur J Radiol*. 2014;83:2007–2012.
25. Sun HY, Lee JM, Shin CI, et al. Gadoxetic acid-enhanced magnetic resonance imaging for differentiating small hepatocellular carcinomas (< or =2 cm in diameter) from arterial enhancing pseudolesions: special emphasis on hepatobiliary phase imaging. *Invest Radiol*. 2010;45:96–103.
26. Huppertz A, Balzer T, Blakeborough A, et al. Improved detection of focal liver lesions at MR imaging: multicenter comparison of gadoxetic acid-enhanced MR images with intraoperative findings. *Radiology*. 2004;230:266–275.